

ESI to accompany:

Peripheral halo-functionalization in [Cu(N[^]N)(P[^]P)]⁺ emitters: their influence on the performances of light-emitting electrochemical cells

Fabian Brunner,^a Laura Martínez-Sarti,^b Sarah Keller,^a Antonio Pertegás,^b Alessandro Prescimone,^a Edwin C. Constable,^a Henk J. Bolink^{*b,c} and Catherine E. Housecroft^{*a}

Fig. S1. Structure of the [Cu(**3**)(xantphos)]⁺ cation.

Fig. S2. Structure of the [Cu(**1**)(POP)]⁺ cation.

Fig. S3. Structure of the [Cu(**1**)₂]⁺ cation.

Fig. S4. Solution absorption spectra of [Cu(N[^]N)(POP)][PF₆] (N[^]N = **1–5**).

Fig. S5. Normalized solid-state emission spectra of [Cu(N[^]N)(POP)][PF₆] (N[^]N = **1–5**).

Fig. S6. Normalized solution (CH₂Cl₂, 2.5 x 10⁻⁵ mol dm⁻³) emission spectra of [Cu(N[^]N)(xantphos)][PF₆] (N[^]N = **1–5**).

Fig S7. Normalized thin film emission spectra of [Cu(N[^]N)(POP)][PF₆] (N[^]N = **1–5**).

Fig S8. Normalized thin film emission spectra of [Cu(N[^]N)(xantphos)][PF₆] (N[^]N = **1–5**).

Fig. S9. EL spectra for LECs.

Fig. S10. Luminance and average voltage versus time for the LEC containing [Cu(**3**)(POP)][PF₆].

Fig S11. Luminance and average voltage versus time for the LEC with [Cu(**4**)(POP)][PF₆].

Fig S12. Luminance and average voltage versus time for the LEC with [Cu(**4**)(xantphos)][PF₆].

Fig. S13. Luminance, average voltage and efficiency in cd A⁻¹ versus time for the LEC with [Cu(**3**)(xantphos)][PF₆].

Fig. S14. Average voltage for glass/ITO/PEDOT:PSS/active layer/Al devices.

Table S1. Photoluminescence lifetimes (τ_{1/2}) for [Cu(N[^]N)(P[^]P)][PF₆] complexes.

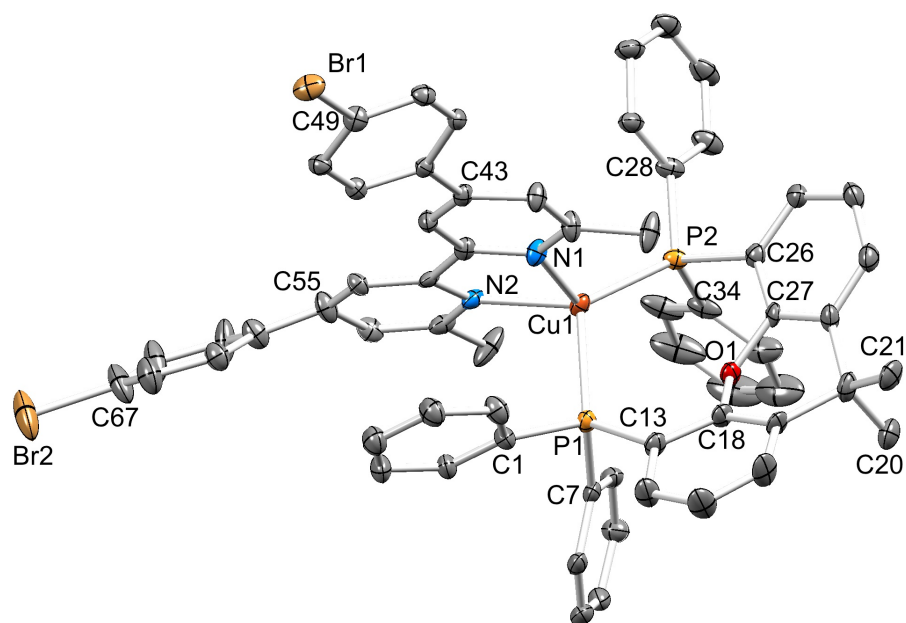


Fig. S1. Structure of the $[\text{Cu}(\mathbf{3})(\text{xantphos})]^+$ cation in $[\text{Cu}(\mathbf{3})(\text{xantphos})][\text{PF}_6] \cdot 0.5\text{H}_2\text{O} \cdot \text{Et}_2\text{O}$ with ellipsoids plotted at the 30% probability level; H atoms are omitted for clarity. The bromophenyl group containing Br2 is disordered and has been modelled over two sites of equal occupancy which share atom C55 in common; only one site is shown. Selected bond parameters: Cu1–P1 = 2.317(3), Cu1–P2 = 2.258(3), Cu1–N1 = 2.080(8), Cu1–N2 = 2.121(8) Å; P1–Cu1–P2 = 117.08(11), P1–Cu1–N1 = 104.2(3), P2–Cu1–N1 = 119.6(3), P1–Cu1–N2 = 100.2(2), P2–Cu1–N2 = 129.3(2), N1–Cu1–N2 = 78.8(3)°.

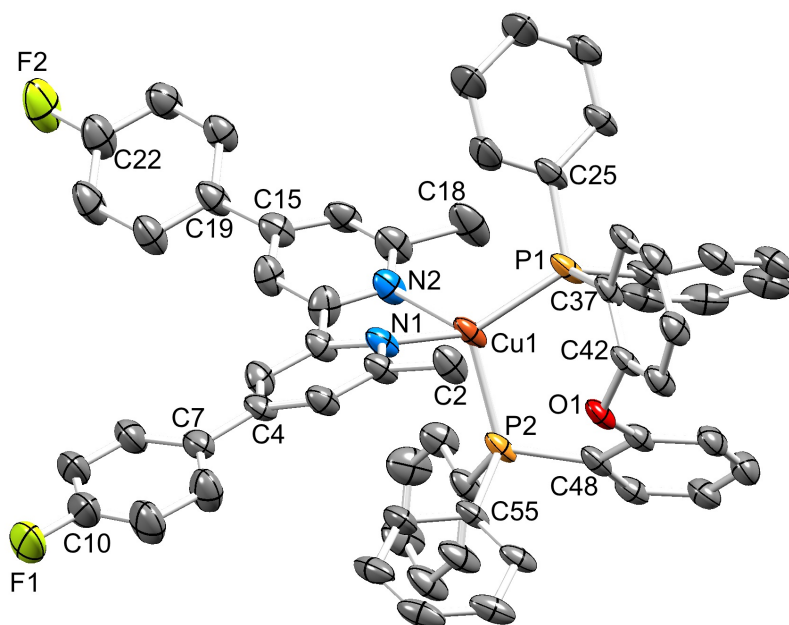


Fig. S2. Structure of the $[\text{Cu}(\mathbf{1})(\text{POP})]^+$ cation in $[\text{Cu}(\mathbf{1})(\text{POP})][\text{PF}_6] \cdot 0.8\text{H}_2\text{O}$ with ellipsoids plotted at the 30% probability level; H atoms are omitted for clarity. The pyridine ring containing N2 and the attached fluorophenyl group containing F2 are disordered and the unit has been modelled over two sites of 0.65:0.35 fractional occupancies; only the major occupancy site is shown. Selected bond parameters: Cu1–N1 = 2.099(6), Cu1–N2 = 2.097(5), Cu1–P1 = 2.2523(15), Cu1–P2 = 2.297(2) Å; N1–Cu1–N2 = 78.5(2), N1–Cu1–P1 = 123.71(15), N2–Cu1–P1 = 120.00(16), N1–Cu1–P2 = 104.32(15), N2–Cu1–P2 = 116.27(17), P1–Cu1–P2 = 110.37(8)°.

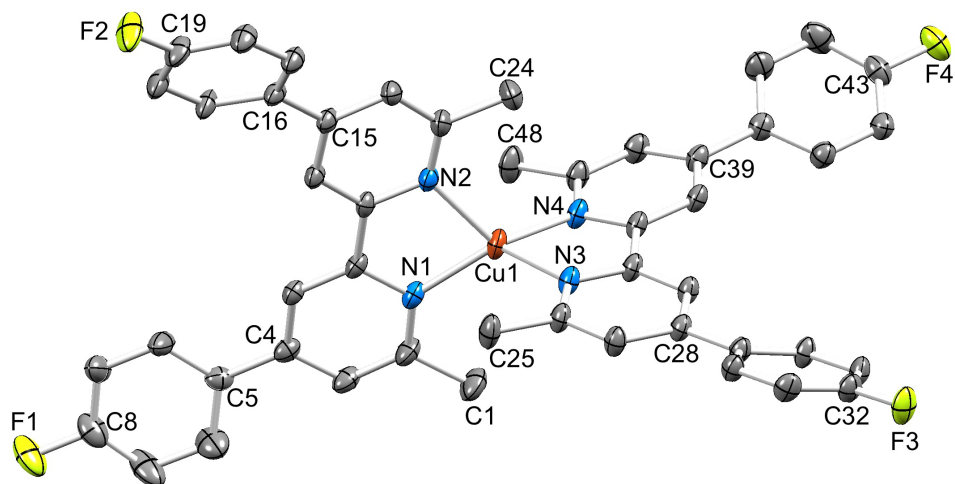


Fig. S3. Structure of the $[\text{Cu}(\mathbf{1})_2]^+$ cation in $[\text{Cu}(\mathbf{1})_2][\text{PF}_6]$ with ellipsoids plotted at the 30% probability level; H atoms are omitted for clarity. Selected bond parameters: Cu1–N2 = 2.044(2), Cu1–N1 = 2.001(2), Cu1–N3 = 2.027(2), Cu1–N4 = 2.000(2) Å; N2–Cu1–N1 = 82.13(9), N2–Cu1–N3 = 117.02(9), N1–Cu1–N3 = 123.42(10), N2–Cu1–N4 = 123.20(10), N1–Cu1–N4 = 133.76(10), N3–Cu1–N4 = 81.89(9)°.

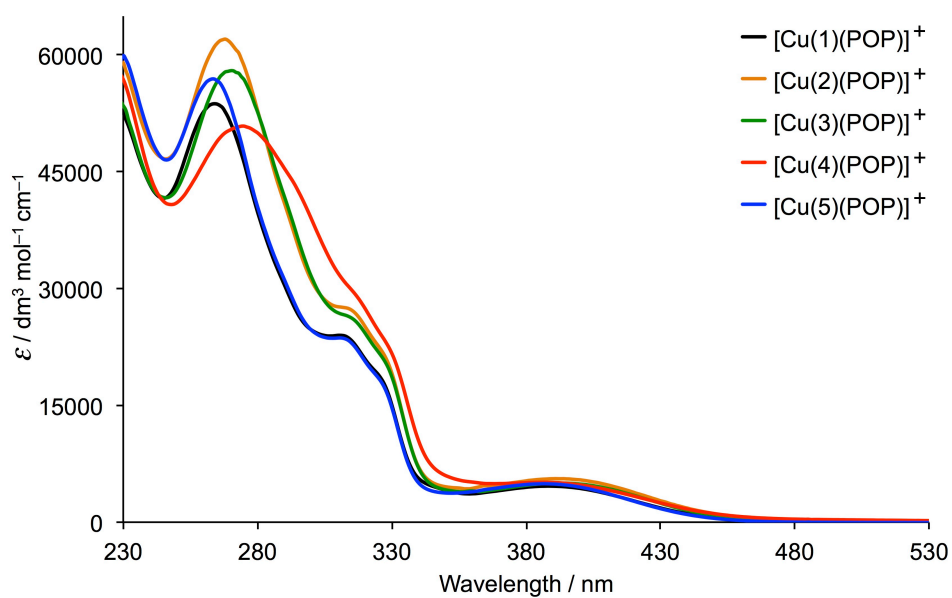


Fig. S4. Solution (CH_2Cl_2 , $2.5 \times 10^{-5} \text{ mol dm}^{-3}$) absorption spectra of $[\text{Cu}(\text{N}^{\text{N}})(\text{POP})]^+[\text{PF}_6]^-$ ($\text{N}^{\text{N}} = \mathbf{1-5}$) complexes.

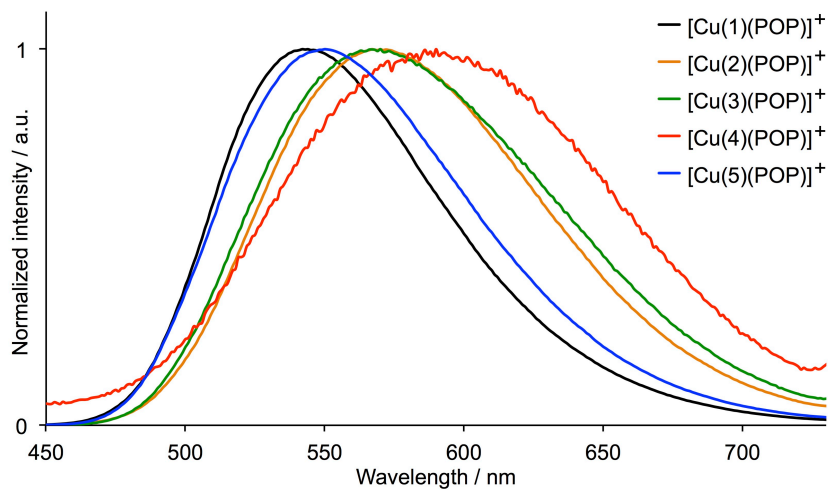


Fig. S5. Normalized solid-state emission spectra of $[\text{Cu}(\text{N}^{\text{N}})(\text{POP})][\text{PF}_6]$ ($\text{N}^{\text{N}} = 1-5$). ($\lambda_{\text{exc}} = 365$ nm).

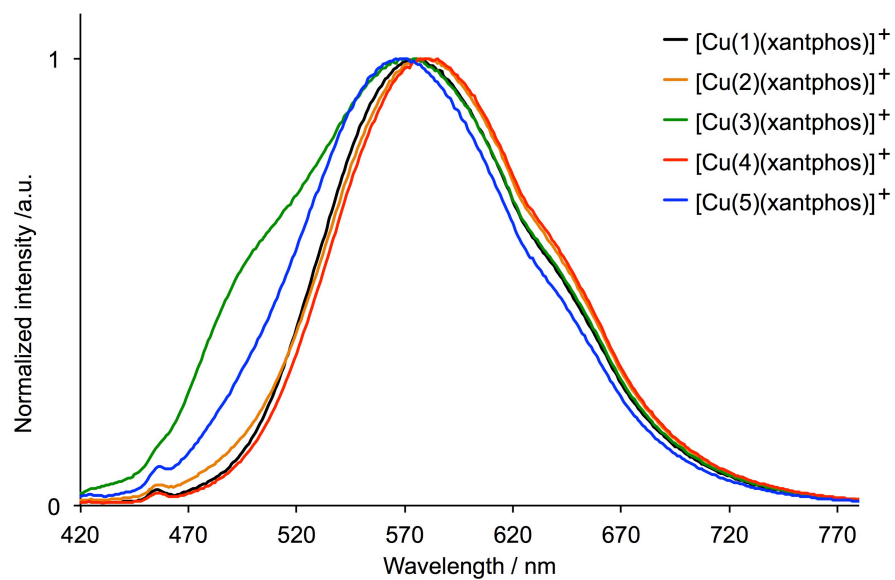


Fig. S6. Normalized solution (CH_2Cl_2 , 2.5×10^{-5} mol dm^{-3}) emission spectra of $[\text{Cu}(\text{N}^{\text{N}})(\text{xantphos})][\text{PF}_6]$ ($\text{N}^{\text{N}} = 1-5$). ($\lambda_{\text{exc}} = 400$ nm).

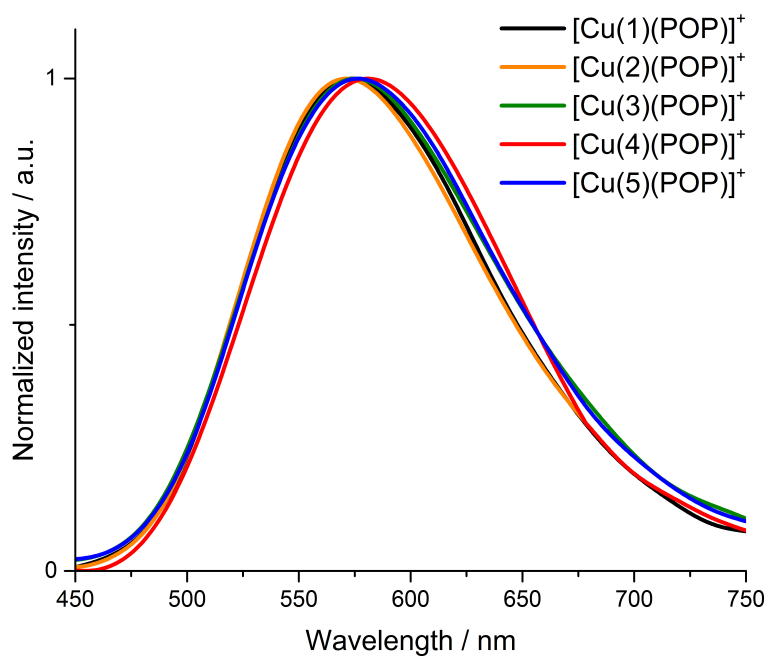


Fig. S7. Normalized thin film emission spectra of $[\text{Cu}(\text{N}^{\wedge}\text{N})(\text{POP})][\text{PF}_6]$ ($\text{N}^{\wedge}\text{N} = 1-5$). ($\lambda_{\text{exc}} = 365$ nm). The thin film consisted of the complex mixed with the ionic liquid 1-ethyl-3-methylimidazolium hexafluoridophosphate.

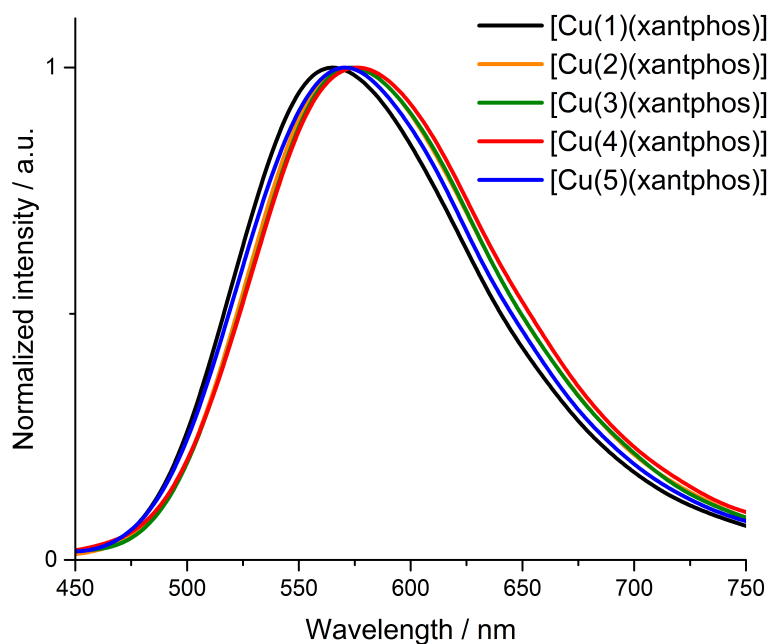


Fig. S8. Normalized thin film emission spectra of $[\text{Cu}(\text{N}^{\wedge}\text{N})(\text{xantphos})][\text{PF}_6]$ ($\text{N}^{\wedge}\text{N} = 1-5$). ($\lambda_{\text{exc}} = 365$ nm). The thin film consisted of the complex mixed with the ionic liquid 1-ethyl-3-methylimidazolium hexafluoridophosphate.

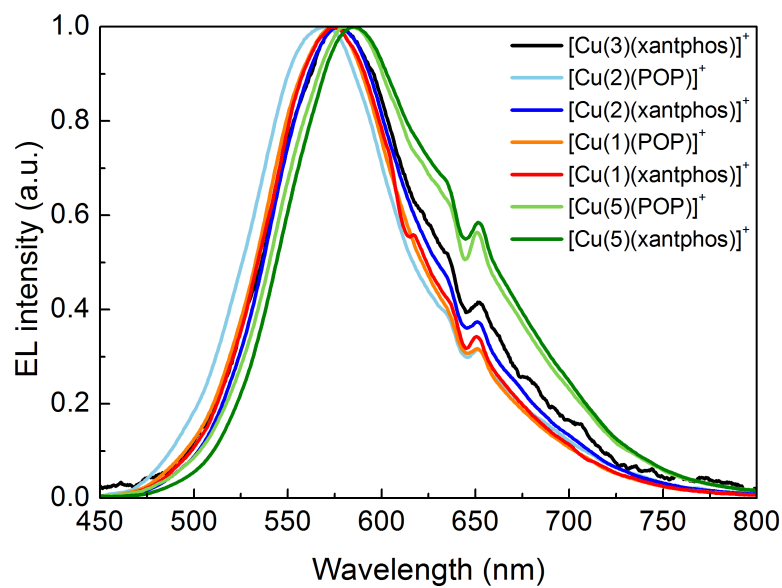


Fig. S9. EL spectra for LECs containing $[\text{Cu}(3)(\text{xantphos})]^+$, $[\text{Cu}(2)(\text{POP})]^+$, $[\text{Cu}(2)(\text{xantphos})]^+$, $[\text{Cu}(1)(\text{POP})]^+$, $[\text{Cu}(1)(\text{xantphos})]^+$, $[\text{Cu}(5)(\text{POP})]^+$ and $[\text{Cu}(5)(\text{xantphos})]^+$.

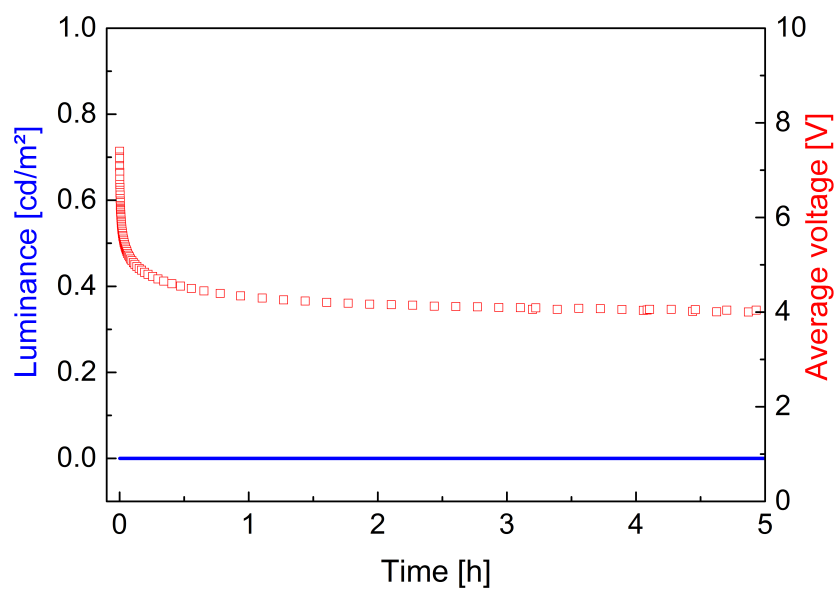


Fig. S10. Luminance (blue line) and average voltage (red symbols) versus time for the LEC with $[\text{Cu}(3)(\text{POP})][\text{PF}_6]$ by applying a block-wave pulsed current of 50 A m^{-2} at a frequency of 1 kHz and a duty cycle of 50%.

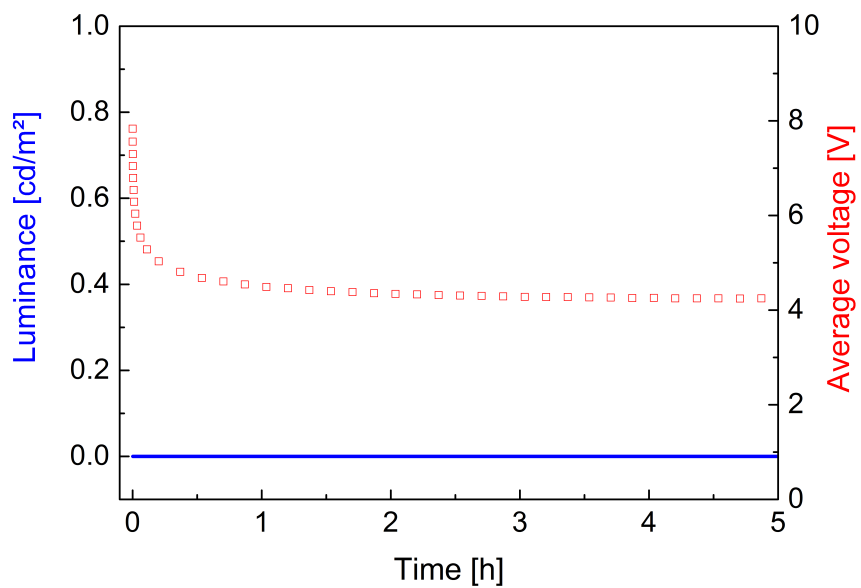


Fig. S11. Luminance (blue line) and average voltage (red symbols) versus time for the LEC with [Cu(4)(POP)][PF₆] by applying a block-wave pulsed current of 50 A m⁻² at a frequency of 1 kHz and a duty cycle of 50%.

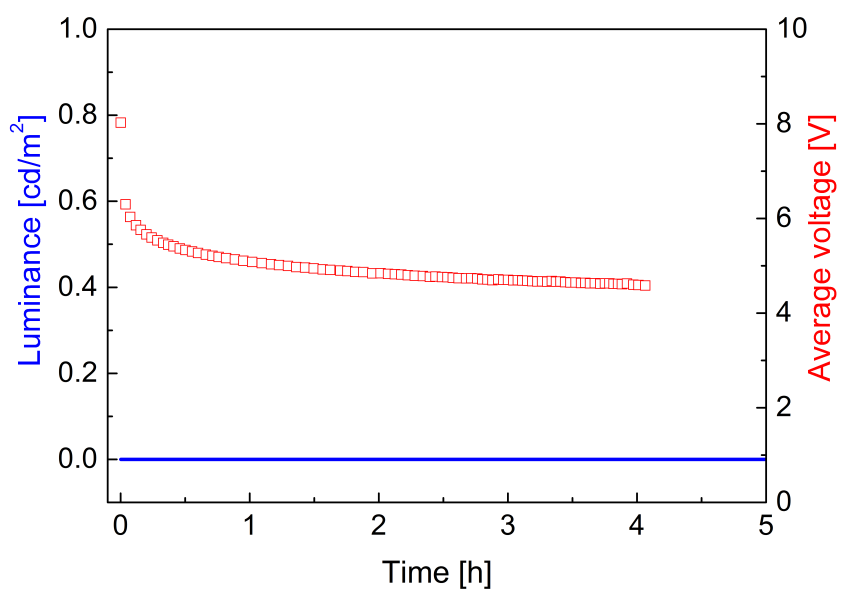


Fig. S12. Luminance (blue line) and average voltage (red symbols) versus time for the LEC with [Cu(4)(xantphos)][PF₆] by applying a block-wave pulsed current of 50 A m⁻² at a frequency of 1 kHz and a duty cycle of 50%.

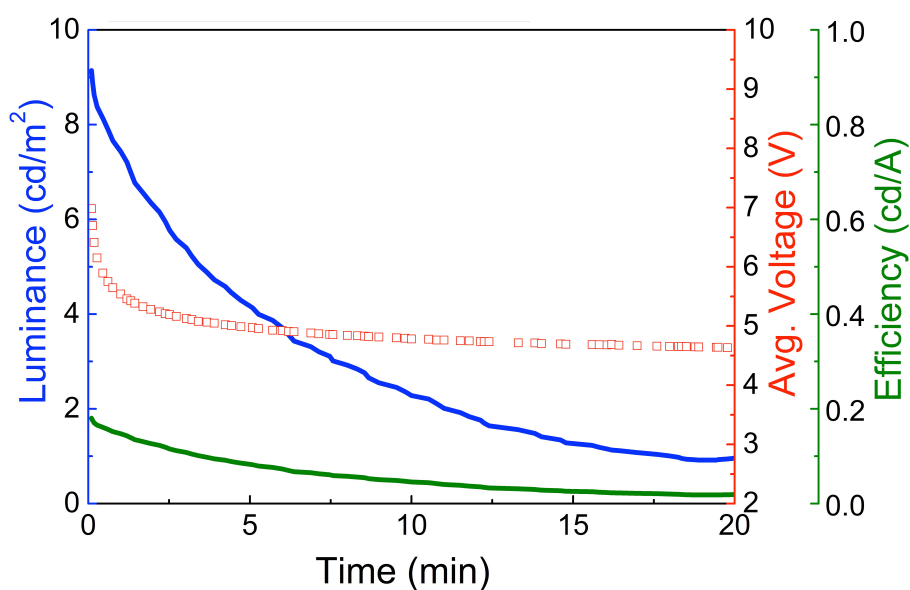


Fig. S13. Luminance (blue line), average voltage (red symbols) and efficiency in cd A^{-1} (green line) versus time for the LEC with $[\text{Cu}(\mathbf{3})(\text{xantphos})][\text{PF}_6]$ by applying a block-wave pulsed current of 50 A m^{-2} at a frequency of 1 kHz and a duty cycle of 50%.

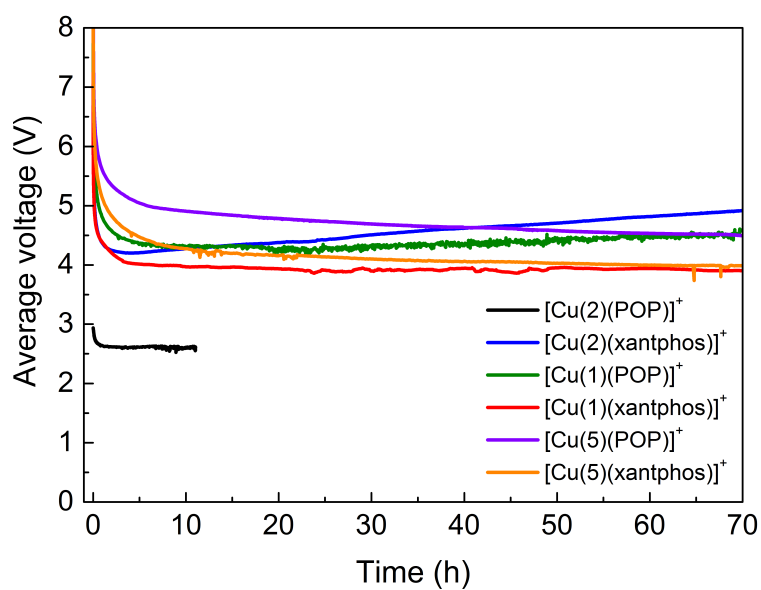


Fig. S14. Average voltage for glass/ITO/PEDOT:PSS/active layer/Al devices measured by applying a block-wave pulsed current of 50 A m^{-2} at a frequency of 1 kHz and a duty cycle of 50%. The active layer consisted of the different $[\text{Cu}(\text{N}^{\wedge}\text{N})(\text{P}^{\wedge}\text{P})][\text{PF}_6]$ ($\text{N}^{\wedge}\text{N} = 1, 2$ and 5) complexes mixed with the ionic liquid 1-ethyl-3-methylimidazolium hexafluoridophosphate.

Table S1. Photoluminescence lifetimes ($\tau_{1/2}$) for [Cu(N^N)(P^{^P})]PF₆ complexes.

Complex cation	CH ₂ Cl ₂ degassed solution ^{a,b}					Powder ^c				
	$\tau_{1/2}(1)$ / μ s	A1	$\tau_{1/2}(2)$ / μ s	A2	$\tau_{1/2}(av)$ / μ s	$\tau_{1/2}(1)$ / μ s	A1	$\tau_{1/2}(2)$ / μ s	A2	$\tau_{1/2}(av)$ / μ s
[Cu(1)(POP)] ⁺	4.5				4.5	11.7	0.9118	1.5	0.05582	11.1
[Cu(2)(POP)] ⁺	4.2				4.2	5.6	0.5335	1.5	0.3531	4.0
[Cu(3)(POP)] ⁺	4.4				4.4	7.1	0.3976	1.6	0.4517	4.2
[Cu(4)(POP)] ⁺	4.1				4.1	2.3	0.2638	0.6	0.4417	1.2
[Cu(5)(POP)] ⁺	4.5	0.4225	1.8	0.504	3.0	11.5	0.8209	1.8	0.1259	10.2
[Cu(1)(xantphos)] ⁺	2.5				2.5	7.2	0.6052	0.8	0.1709	5.8
[Cu(2)(xantphos)] ⁺	2.8				2.8	7.0	0.5854	1.9	0.3025	5.2
[Cu(3)(xantphos)] ⁺	2.8				2.8	8.3	0.5975	1.9	0.3223	6.1
[Cu(4)(xantphos)] ⁺	2.6				2.6	4.7	0.4578	1.2	0.4559	3.0
[Cu(5)(xantphos)] ⁺	3.7				3.7	7.2	0.6728	1.6	0.2477	5.7